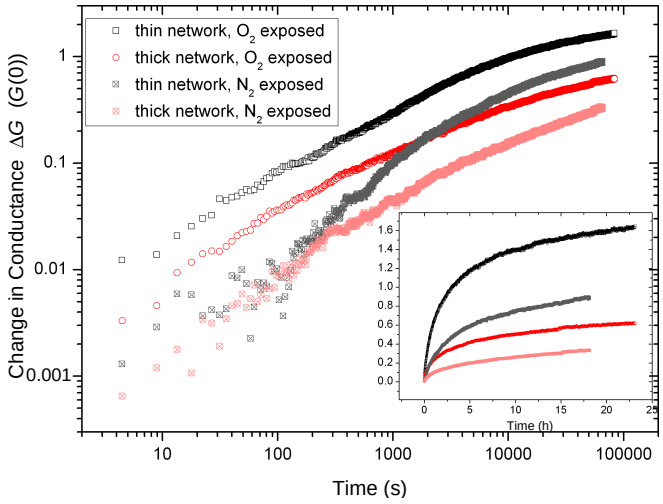

FIG. 2: (Color online) Fractional change in conductance $\Delta G = G/G(0) - 1$ versus time t in seconds and hours (inset) following exposure to O_2 and N_2 for thin (□, ⊠) and thick (○, ⊗) SWNT networks respectively, on log-log and linear (inset) scales (Refs. 8 and 9).

exposure for thick and thin SWNT networks. These samples were initially placed under vacuum ($\sim 1 \times 10^{-6}$ mbar) and irradiated by a UV light-emitting diode (LED) ($\lambda \sim 400$ nm) at low intensity ($\sim$0.03 mW/cm^2) for approximately 12 h to desorb surface and interbundle adsorbates (surface dopants) from the SWNTs. Once the SWNT network's conductance stabilized, the samples were exposed to either O_2 (99.5% pure) or N_2 (99.998% pure) at 1 atm. The conductance of the samples was then monitored by periodically sampling ($\Delta t \approx 1$ s) the current while applying a fixed bias of 1 mV to the thick (metal-like) SWNT network ($R \approx 1$ kΩ) and 10 mV to the thin (semiconductor-like) SWNT network ($R \approx 1000$ kΩ), as shown in Fig. 2.

After 5 min of exposure to O_2, the thin network shows an increase in conductance of about 13% while the thick network's conductance changes by about 7%. For the same exposure to N_2, both networks show substantially smaller conductance changes of 2%–3%. However, at exposure times of more than 2 h, the thin SWNT network response to N_2 is similar to that of the thick SWNT network to O_2. This might be caused by a weaker physisorption of N_2 to the SWNT networks than O_2. The inset of Fig. 2 also shows that at very long exposure times the fractional change in conductance, $\Delta G = G/G(0) - 1$, becomes saturated after 24 h. Further, the response to O_2 depicted in Fig. 2 shows that the conductance change for a thin SWNT network is about two to three times that of the thick SWNT network at all times. This suggests that the conductance change under O_2 exposure is an intrinsic property of the SWNT networks, present even at very low O_2 concentrations. Herein we shall focus on the microscopic origin of the network sensitivity to O_2 and N_2, with the temporal behavior of the networks discussed elsewhere.[8,9]

We have performed the Raman spectroscopy to characterize our SWNT network samples, which were produced via

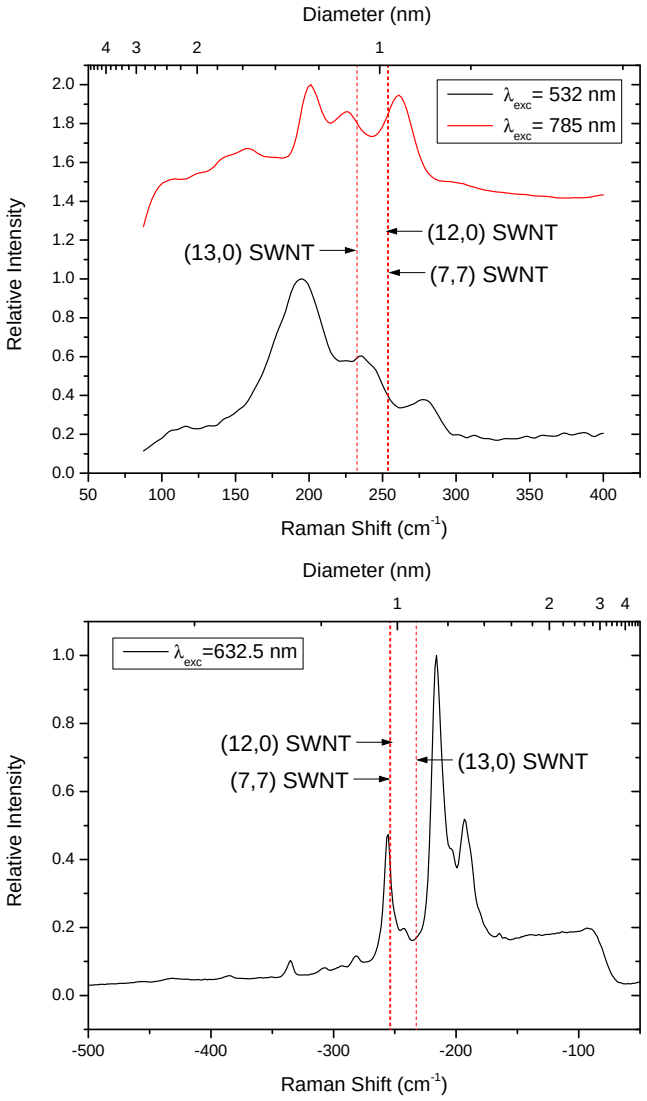

FIG. 3: (Color online) Raman spectra and approximate diameter distribution of HiPco SWNT sample for an excitation wavelength (top) $\lambda_{exc} \approx 532$ nm (lower black curve), $\lambda_{exc} \approx 785$ nm (upper red curve), and (bottom) $\lambda_{exc} \approx 632.5$ nm (——). The DFT calculated diameters of $d \approx 9.76$ Å, 9.79 Å, and 10.66 Å for (7,7), (12,0), and (13,0) SWNTs, respectively, are provided for comparison (dashed lines).

the high-pressure carbon monoxide (HiPco) method. Figure 3 shows the radial breating mode (RBM) Raman signals of HiPco samples at excitation wavelengths $\lambda_{exc} \approx 532$ nm, $\lambda_{exc} \approx 632.5$ nm and $\lambda_{exc} \approx 785$ nm. The van Hove singularity energy separation was calculated using the tight-binding approximation with the carbon-carbon interaction energy $\gamma_0 \approx 2.9$ eV and carbon-carbon bond length $a_{C-C} \approx 1.44$ Å. The SWNT diameter d dependence of the RBM frequency ν_{RBM} for isolated SWNTs on SiO_2 has been shown[26] to behave as $\nu_{RBM} \approx 248/d_t$. The DFT calculated diameters for (7,7), (12,0), and (13,0) SWNTs of $d \approx 9.76$, 9.79, and 10.66 Å, respectively, are found to correlate well with the HiPco Raman shift, as shown in Fig. 3. This should ensure a good de-